RESONANCE CONTROL FOR NARROW BANDWIDTH PIP-II CAVITIES

J. Holzbauer#, Y. Pischalnikov, W. Schappert. - FNAL, Batavia, IL 60510, USA

Abstract

The PIP-II project at FNAL calls for a SRF pulsed proton driver linac to support the expanding neutrino physics program including DUNE/LBNF. The relatively low beam current and high quality factors called for in the design means that these cavities will be operated with small RF bandwidths, meaning that they will be sensitive to microphonics. Combined with a 20 Hz pulsed operational structure and the use of four different, complex cavity geometries means that resonance control will be extremely challenging. Work is ongoing at FNAL to develop active resonance stabilization techniques using fast piezoelectric tuners in support of PIP-II. These techniques as well as testing and development results using a prototype, dressed low-beta single-spoke cavity will be presented along with an outlook for future efforts.

PIP-II PROTOTYPE CAVITY

An extensive design and prototyping effort at Fermilab has been focused on a 325 MHz single spoke resonator for the PIP-II project. The cavity has been optimized for performance, multipacting minimization, and pressure sensitivity. Integrated tests have demonstrated functionality of the dressed cavity with tuner and high-power coupler.

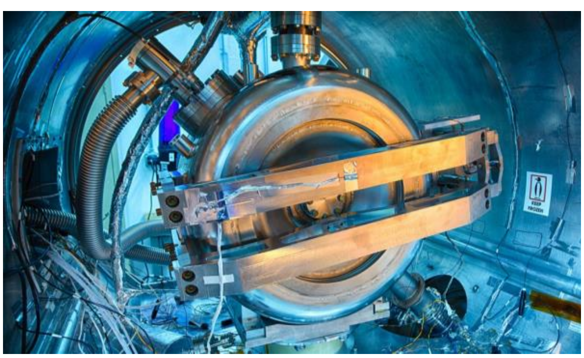

Figure 1: Dressed Single Spoke Resonator with tuner and high-power coupler installed in the Spoke Test Cryostat at Fermilab.

This resonator is designed to operate at 2 K. PIP-II calls for a pulse structure with a 0.5 ms flattop at 12.5 MV/m, 20 Hz repetition rate, and 15% duty cycle. The coupler is designed for operation over several kW with a half bandwidth of 30 Hz. Tuning is accomplished via a single lever tuner attached to the helium vessel, acting on one beam pipe [1]. The motor is actuated via a slow motor for course tuning over large range and two piezo tuners encapsulated in such a way to act together, but still remain functional is one piezo fails. After installation in the Spoke Test Cryostat (STC) seen in Figure 1 and cooldown, the tuner is designed and set to remain barely out of contact with the cavity. The slow motor moved the tuner into contact with the cavity and preload the piezo and tuner. For the following testing, the tuner was loaded and left at the low loading end of the operating tuning range.

The prototype coupler gave an initial half bandwidth of 142 Hz (Loaded Q of 1.15e6). An RF reflector was installed to narrow the cavity bandwidth, giving a final Loaded Q of 5.24e6 (31 Hz half bandwidth).

RF DEVELOPMENT CIRCUIT

Development was done on an FPGA based digital RF system (seen in Figure 2). Direct RF signals are downconverted to 13 MHz via narrowband, analog downconverter. These signals are then digitized at the eighth harmonic, 104 MHz, by 14-bit ADCs.

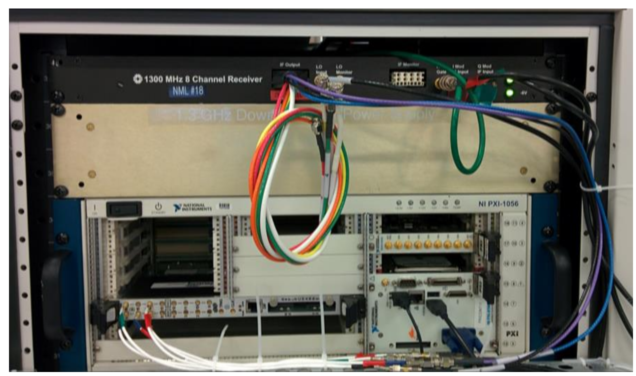

Figure 2: Analog downconverter, RF transceiver, and FPGA-based RF controller.

IF I/Q signals and piezo drive are calculated in the FPGA and generated by 14-bit DACs. IF signals are analog upconverted to RF frequency and sent to the high power amplifier. Monitoring, logging, and setting of registers is done via on-board PC controller. Piezo signal was amplified by a low-noise PiezoJena amplifier up to 150 Volts.

$$\frac{dP}{dt} = -(\omega_{1/2} + i\delta)P + 2\omega_{1/2}F$$

$$\omega_{1/2} = -\frac{\left\langle \mathrm{Re}\left(P^*\left(\frac{dP}{dt}\right)\right)\right\rangle}{\left\langle \mathrm{Re}\left(P^*(P-2F)\right)\right\rangle}$$

$$\delta = -\frac{\mathrm{Im}\left(P^*\left(\frac{dP}{dt} - 2\omega_{1/2}F\right)\right)}{P^*P}$$

Equation 1: Separation of the baseband envelope into real and imaginary parts which allows direct calculation of the cavity half bandwidth and detuning.

DETUNING CALCULATION

Once digitized, signals are digitally downconverted to baseband. Cavity detuning can be determined from these complex baseband cavity signals. The complex equation for baseband envelope can be separated into two real equations, one for the cavity half bandwidth and one for the detuning, seen in Equation 1.

Precision, online calculation of detuning is required for all successful feedback efforts. This effort fell into two major categories: correcting systematic effects and calibrations of the incoming signals, and proper online calculation of detuning.

$$\frac{Z_T I_{Forward}}{V_{Cavity}} = \frac{1}{2}\left(1 + \frac{Q_{Ext}}{Q_{Int}} + i\frac{\omega' - \delta}{\omega_X}\right)$$

$$\frac{Z_T I_{Reflected}}{V_{Cavity}} = \frac{1}{2}\left(1 - \frac{Q_{Ext}}{Q_{Int}} - i\frac{\omega' - \delta}{\omega_X}\right)$$

Equation 2: Forward to probe, and reflected to probe transfer functions.

The ratio of the complex forward/probe and reflected/probe signals are linear functions of detuning (see Equation 2). Sweeping detuning of the RF drive, either by frequency modulation of a fixed frequency system or loop phase of a locking circuit like phase-lock or self-excited loop scans the transfer function phase space. The self-consistency condition from the transfer function means that the sum of these transfer functions must sum to unity, with the slopes with respect to detuning being purely imaginary and opposite [2]. An example of a calibrated phase scan can be seen in Figure 3.

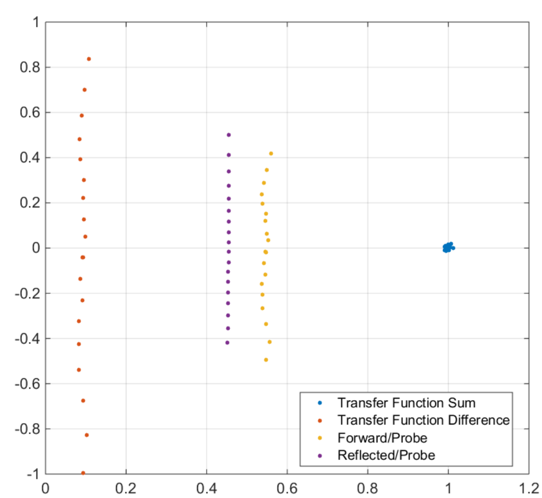

Figure 3: Calibrated forward/probe and reflected/probe transfer functions, including sum (should be unity) and difference (whose real part is proportional to inverse beta).

Satisfying these self-consistency conditions give the relative calibration of forward to probe and reflected to probe signals. The real part of the difference of transfer functions gives inverse beta, and decay time gives the loaded Q. The final absolute calibration of the probe signal (and thus gradient) requires comparison to a reference signal in the more traditional fashion.

Using these techniques, the systematic errors in the RF circuits can be studied and corrected [3]. These errors include reflections from the circulator, imperfect directivity in the directional coupler, and off-resonance errors.

Calculating the detuning online is also a challenging task. This is mostly because of the significant noise associated with the derivative terms. Careful effort is required to filter this high frequency noise and calculate a realistic detuning online. Planned upgrades of this system include use of a Kalman Filter to provide an optimal calculation of detuning.

DETUNING COMPENSATION TECHNIQUES

Narrow bandwidth SRF cavities can have Lorentz Force Detuning (LFD) significantly larger than their bandwidth. This leads to Pondermotive instabilities at operating gradient, which caused the cavity to fall sharply off of resonance when disturbed by microphonics.

LFD is proportional to the gradient squared. This was compensated for by mixing the probe signal with itself, scaling properly, and applying this signal to the piezo tuner. The process of tuning this feedforward signal can be seen in Figure 4.

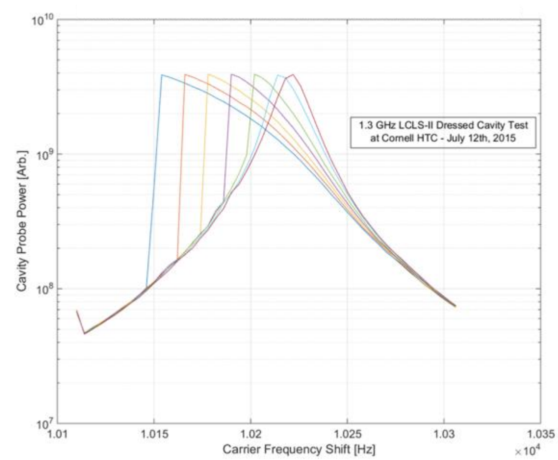

Figure 4: Sweeping of the cavity resonance from high frequency to low for different LFD compensation coefficients. Optimal compensation symmetrizes the resonance.

While the cavity testing environment is designed to minimize mechanical vibration and noise to the cavity, residual microphonics detuning is inevitable. Proportional, broadband feedback of detuning was found to be of limited use due to excitation of resonance in the cavity/tuner system. A filter bank was built, using narrowband filters to extract different spectral components of the detuning signal. The individual frequencies and bandwidths of the filter bank channels were tuned manually based on observation of the cavity detuning.

ISBN 978-3-95450-169-4

The PIP-II cavity operation is specified to be an aggressive pulse schedule. During research at Fermilab for the ILC, an adaptive feedforward algorithm was developed to compensate for the deterministic noise caused by the RF pulse [4]. The basis of this technique is a characterization of the cavity with a time-domain transfer function through the pulse structure. The pulses, an example of which can be seen in Figure 5, are done in both positive and negative directions. The difference of these signals gives the Transfer Function by rejecting the background microphonics detuning.

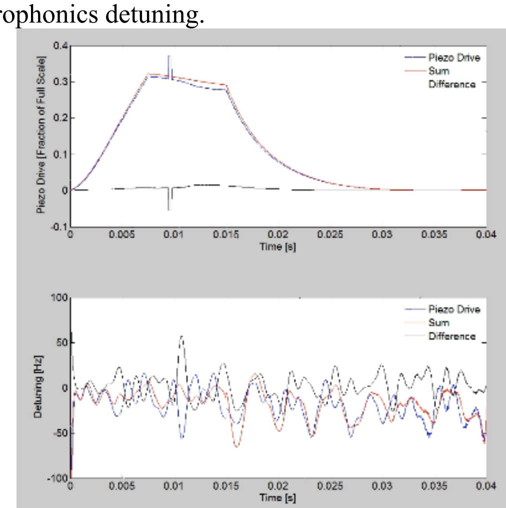

Figure 5: RF pulse with one of the piezo pulse superimposed. The piezo pulses sweep through the RF pulse.

This transfer function, constructed from a series of discrete impulses, can be inverted to create a proper compensation waveform for a given detuning. Numerical instabilities can be suppressed using singular value decomposition or Tikhionov Regularization. The effects of this algorithm can be seen in Figure 6.

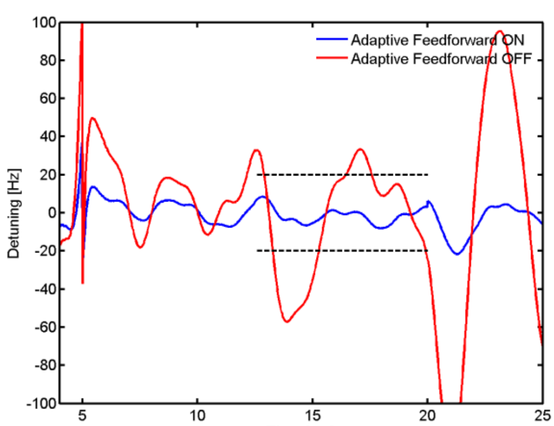

Figure 6: Typical detuning over the RF pulse with and without Adaptive Feedforward compensation. Compensation is active for the rise and fall time in addition to the flattop. The dashed lines indicate both flat top time and detuning specification.

COMPENSATION PERFORMANCE

Compensation development was done first in CW and then in pulsed mode. Because of firmware limitations, a 25 Hz repetition rate was used with a 7.5 ms flattop at a gradient exceeding the PIP-II specification. The results of the three compensation schemes operating together can be seen in Figure 7.

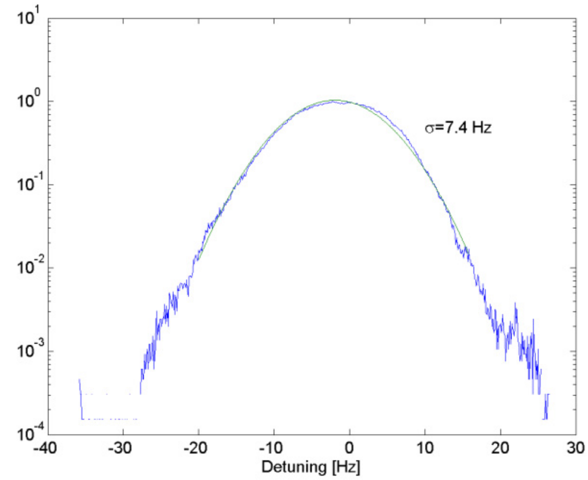

Figure 7: Histogram of the peak detuning by pulse. The remaining detuning is Gaussian with an RMS detuning of 7.4 Hz.

CONCLUSION

The resulting detuning (7.4 Hz RMS), while roughly an order of magnitude better than without compensation, is still almost a factor of two higher than required for PIP-II. Future improvements include implementation of a Kalman filter for accuracy and automation of optimal filter bank coefficients based on the transfer function generated by the adaptive algorithm characterization.

REFERENCES

[1] D. Passerelli *et al.*, "Performance of the Tuner Mechanism for SSR1 Resonators During Fully Integrated Tests at Fermilab.", SRF 2015, THPB061.

[2] O. Melnychuk *et. al.*, "Phase Method of Measuring Cavity Quality Factor." , IPAC2014, WEPRI05.

[3] J.P. Holzbauer *et. al.*, "Systematic Uncertainties in RF-Based Measurement of Superconducting Cavity Quality Factors.", NIM-A, Volume 830, 11 September 2016, pp. 22-29.

[4] W. Schappert *et. al.* "Adaptive Compensation for Lorentz Force Detuning in Superconducting RF Cavities.", SRF2011, FRIOA01.